Density Functional Theory Study on the Selective Reductive Amination of Aldehydes and Ketones over Their Reductions to Alcohols Using Sodium Triacetoxyborohydride

Shannon J. Oliphant and Robert H. Morris*

Read Online

ACCESS | Metrics & More | Article Recommendations | SI Supporting Information

ABSTRACT: Reductive amination is one of the most important methods to synthesize amines, having a wide application in the pharmaceutical, fine chemicals, and materials industries. In general, the reaction begins with dehydration between a carbonyl compound and an amine compound, forming an imine, which is then reduced to an alkylated amine product. Sodium triacetoxyborohydride (STAB) is a popular choice for the reducing agent as it shows selectivity for imines over aldehydes and ketones, which is particularly important in direct reductive amination where the imine and carbonyl compounds are present concurrently. Here, we analyze the reaction pathways of acid-catalyzed direct reductive amination in 1,2-dichloroethane (DCE) with acetaldehyde and methylamine. We find that the transition states for the formation and subsequent reduction of Z-methylethylideneimine (resultant aldimine from acetaldehyde and methylamine) have lower energies than the reduction of acetaldehyde. Transition state structures for the hydride transfers are organized by the Lewis-acidic sodium ion. Additionally, reduction reactions with formaldehyde and acetone and their imine derivatives (with methylamine) are investigated, and again, the hydride transfer to the resultant aldimine or ketimine is lower in energy than that of their parent carbonyl compound.

ΔG‡ = 24.1 kcal/mol ΔG‡ = 10.6 kcal/mol

Hydride transfer between STAB and Aldehyde or Imine
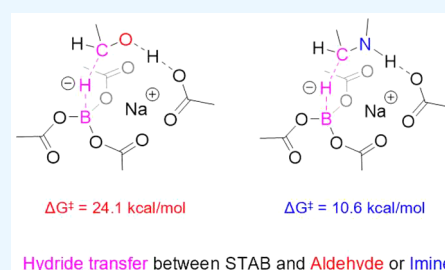
INTRODUCTION

Reductive amination is one of the most important methods to synthesize amines, having a wide application in the pharmaceutical,[1] agricultural,[2] and materials[2] industries. Regarding pharmaceuticals, nearly one-fourth of all C−N bond-forming reactions are performed via reductive amination.[3,4] In general, the reaction begins with dehydration between a carbonyl compound and an amine compound to form an imine, which is then reduced to an alkylated amine product (Scheme 1).[5] Direct reductive amination, wherein formation of the imine and subsequent reduction occur in situ, presents a convenient one-pot synthesis method to produce alkylated amines. Under these reaction conditions, the choice of reducing agent is crucial as it must selectively reduce the imine over the carbonyl compound starting material.[6] Thus, sodium triacetoxyborohydride (STAB) is a popular choice for reducing agent as it shows selectivity for imines over aldehydes and ketones, unlike other reducing agents.[6,7] This selectivity for imines has been exploited in many synthesis protocols, such as within drug patents for cinacalcet,[8,9] lapatinib,[10] and pramipexole,[11] which all use reductive amination between an aldehyde and a primary amine at one step of their synthesis. The selectivity exhibited by STAB is postulated to be attributed to the three acetoxy groups, as they can stabilize the B−H bond via steric shielding and electron-withdrawing effects.[12] However, to our knowledge, there is no report in the literature that computationally probes the selectivity of STAB.

Herein, density functional theory (DFT) methods are used to clarify the energetic favorability of imine reduction over aldehydes and ketones via STAB.

Computational studies in the literature related to reductive amination largely focus on transition metal catalysis and not necessarily commonly used synthetic protocols. DFT has been used to probe the mechanisms of reductive amination utilizing cobalt,[13] nickel,[14] iridium,[15] osmium,[16] and rhodium[17] catalysts. These studies focus on homogeneous catalysis utilizing molecular hydrogen as the reducing agent, apart from the iridium and osmium catalyst studies. Balcells et al.[15] analyzed iridium-catalyzed reductive amination with an alcohol oxidation mechanism to provide a hydride source, while Vinogradov et al.[16] investigated osmium catalysis with carbon monoxide as the reducing agent. However, few studies have computationally probed systems that do not contain transition metal catalysts, with even fewer studies analyzing boron complexes. In the study of Zhao et al.,[18] DFT was used to examine the reaction mechanisms of borane-catalyzed reductive amination between benzaldehyde and aniline, with

Scheme 1. General Reductive Amination Reaction Scheme where R^1 and R^3 Can Be Alkyl or Aryl and R^2 Can Be Alkyl or Hydrogen[a]
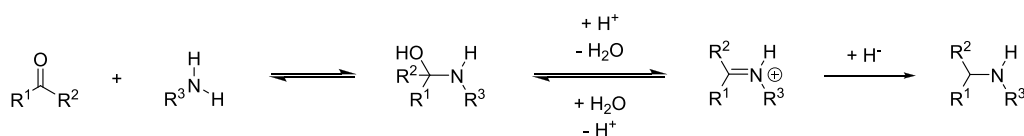
[a]The starting materials for the carbonyl compound are most commonly aldehydes or ketones, while primary amines or ammonia can be used for the amine compound. Secondary amines can also be used for reductive amination; however, they can condense to form an enamine, rather than an imine. Reducing agents (hydride source) are typically catalytic hydrogenation (H_2) or borohydride complexes ($NaBH_4$, $NaBH_3CN$, and $NaBH(OAc)_3$). Reductive amination is often done under slightly acidic conditions, with acetic acid (AcOH) being the most common choice for the proton source.

molecular hydrogen as the reducing agent and tetrahydrofuran (THF) as the solvent. Their results showed that the product of this reaction varied depending on the nature of the Lewis acid catalyst (borane complexes) and could in fact be controlled by adjusting the natural charge on the boron atom. Additionally, in the study of Narvariya et al.,[19] the reductive amination of benzaldehyde and aniline was studied in the Brønsted acidic ionic liquid triethylammonium hydrogen sulfate [Et_3NH]-[HSO_4], with sodium borohydride as the reducing agent. They found that the hydrogen sulfate anion of the ionic liquid played a critical role in catalyzing the reaction, assisting in both geometry optimization and water elimination. With these studies, acidic species play a significant role in reduction amination when boron complexes are implemented, an important consideration when analyzing STAB selectivity.

As previously stated, there appears to be no report in the literature that computationally probes the selectivity of STAB in the reduction of imines over aldehydes or ketones. The aim of this computational research is to explain the selectivity of STAB in reductive amination protocols that are commonly applied in the laboratory. When STAB is utilized in reductive amination, typically, the preferred solvent is DCE, with less frequent use of THF, and acetic acid is the common choice for the catalyst.[6] Thus, the reaction pathways of acetic acid-catalyzed direct reductive amination in DCE with acetaldehyde and methylamine were investigated (Scheme 2), with

Scheme 2. Investigated Direct Reductive Amination Protocol, where R^1 and R^2 Can Be Alkyl or Hydrogen[a]
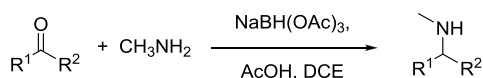
[a]Later investigations in this report will analyze the reduction reaction in THF and exchange Na^+ with Li^+ and K^+.

elucidation of plausible mechanisms of the transition states and their respective energies. The reaction between acetic acid and STAB was not investigated because STAB is regularly used in excess; thus, such a reaction in the low dielectric constant solvent DCE or THF will not compete with the reductive amination.[6,7]

The results suggest that the formation and subsequent reduction of Z-methylethylideneimine (resulting from the condensation of acetaldehyde and methylamine) were favored over the straight reduction of acetaldehyde. Regarding the located transition states, it appears that Brønsted–Lowry and Lewis acids played pivotal roles by assembling the reactant geometry and providing a proton source. Additionally, reduction reactions with formaldehyde and acetone, and

their respective imines, were analyzed (Scheme 2), and again, it was found that imine reduction was favored over the reduction of the parent carbonyl compound. Further investigation into solvent and Lewis acid effects saw the solvent choice having a greater impact on molecular geometry, while the Lewis acid choice affects the reaction energetics significantly.

◼ COMPUTATIONAL DETAILS

All DFT calculations were carried out with the Gaussian 16 package[20] and the M062X functional[21] in conjunction with the basis set 6-311+G(d,p). All calculations were performed at the standard state (298.15 K, 1 atm) and used the SMD solvation model.[22] The frequency analysis was calculated at the same level of theory as the geometry optimization, with the free energies taken directly from the Gaussian output. Transition states were located with the qst2 or qst3 methods and confirmed with intrinsic reaction coordinate (IRC) calculations.[23,24]

◼ RESULTS AND DISCUSSION

Complete Reaction Pathways of Acid-Catalyzed Reductive Amination between Acetaldehyde and Methylamine in the DCE Solvent. Direct reductive amination requires the in situ imine formation and subsequent reduction to be both favored over the carbonyl compound reduction. To investigate the experimentally observed imine selectivity of STAB, calculations of the possible reaction pathways in a direct reductive amination protocol were performed utilizing acetaldehyde and methylamine as the carbonyl and amine compound representatives, respectively. These reaction pathways included the formation and subsequent reduction of Z-methylethylideneimine (the aldimine formed by condensation of acetaldehyde and methylamine) and the reduction of acetaldehyde. The formation of E-methylethylideneimine was not investigated as the reduction of the (Z)-isomer was found to have a 0.4 kcal/mol lower activation barrier than that of the (E)-isomer. In addition, acetic acid was used as the acid catalyst and DCE as the solvent.

The formation of Z-methylethylideneimine is an exergonic reaction arising from the condensation of acetaldehyde and methylamine (Figure 1). The condensation reaction begins with the formation of 1-methylaminoethanol, the hemiaminal derived from acetaldehyde, methylamine, and acetic acid (1). The initial transition state ($TS_{1\rightarrow2}$) entails the concerted formation of the C–N bond and protonation of carbonyl oxygen. After the initial transition state, the reaction pathway falls to an adduct between the protonated hemiaminal and
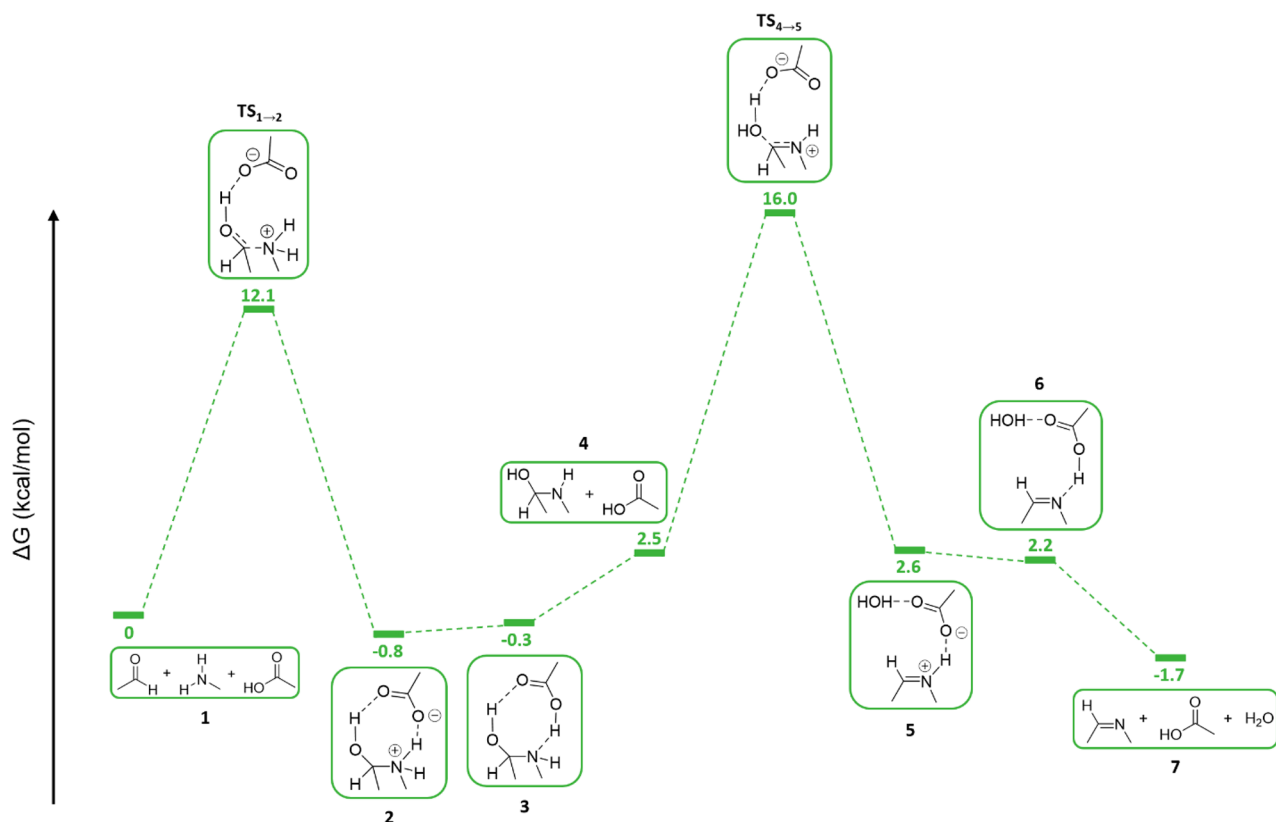
Figure 1. Reaction coordinate diagram for the condensation of acetaldehyde and methylamine in DCE. The condensation reaction forms Z-methylethylideneimine.

acetate (**2**). While in the adduct, a barrierless proton transfer occurs from the nitrogen to the oxygen in the acetate, forming the hemiaminal and regenerating the acetic acid (**3**). DFT calculations of this proton transfer confirm that the free energy and enthalpy values of the transition state are within the error of a barrierless transfer (see Figure S1 in the Supporting Information). After the adduct separates, the reaction pathway proceeds upward toward the hemiaminal intermediate (**4**), which is higher in energy than the starting materials. This higher energy value is expected as hemiaminals are rarely observed in experiment.[25] The rise in energy leads into the second transition state (**TS$_{4 \to 5}$**), where water is removed from the hemiaminal. The water elimination step involves two processes: the protonation of the hydroxyl oxygen and breakage of the C−O bond. This is the rate-determining step (RDS) for the entire imine-forming reaction, an observation that is supported by studies of imine synthesis in water.[26,27] They found that water elimination becomes the RDS when the solution pH is above 4, which would be similar to conditions explored in the DFT calculations considering the use of acetic acid (pK_a = 4.76 in water and 15.5 in DCE relative to picric acid[28]). After water is removed, the reaction pathway falls to another adduct between the Z-methylethylideneiminium and acetate (**5**). Again, a barrierless proton transfer occurs from the nitrogen in the Z-aldiminium to the oxygen in the acetate, regenerating the acetic acid and forming Z-methylethylideneimine (**6**). DFT calculations confirm that this proton transfer is also barrierless (see Figure S2 in the Supporting Information). The final state sees the separation of the adduct, with the Z-aldimine, acetic acid, and water

occupying the lowest free energy position in the reaction pathway (**7**).

There are two possible reduction reactions (Figure 2) in a direct reductive amination protocol with acetaldehyde and methylamine: reduction of the Z-aldimine (represented in purple) and reduction of the acetaldehyde (represented in red). Continuing from the imine formation reaction pathway (represented in green), the reduction of the Z-aldimine sees the substrate accepting the hydride from STAB in the transition state (**TS$_{7 \to 8}$**). After the hydride is transferred, the reaction pathway falls in energy to the ending complex between the alkylated amine product, sodium acetate, and triacetoxyboron (**8**). Regarding the acetaldehyde reduction, it also accepts the hydride from STAB in the transition state (**TS$_{7 \to 8}$**), yielding the ending complex with the alcohol product, sodium acetate, and triacetoxyboron (**8**).

Based on these calculations, the formation and reduction of the Z-aldimine are more thermodynamically and kinetically favored over the reduction of acetaldehyde. All the transition states in the Z-aldimine reaction pathway were found to have a lower activation free energy than the activation free energy of the acetaldehyde reduction. Moreover, the free energy of reaction for the hydride addition, the final step in the reaction pathway, was lower in the Z-aldimine case than in the acetaldehyde. Thus, these results support experimental findings that, in a direct reductive amination protocol utilizing STAB, acetaldehyde will condense faster with methylamine than react directly with STAB.

The factors that determine the selectivity for hydride transfer are subtle and do not entail the typical explanations of charge distribution nor deformation energy. The charge on
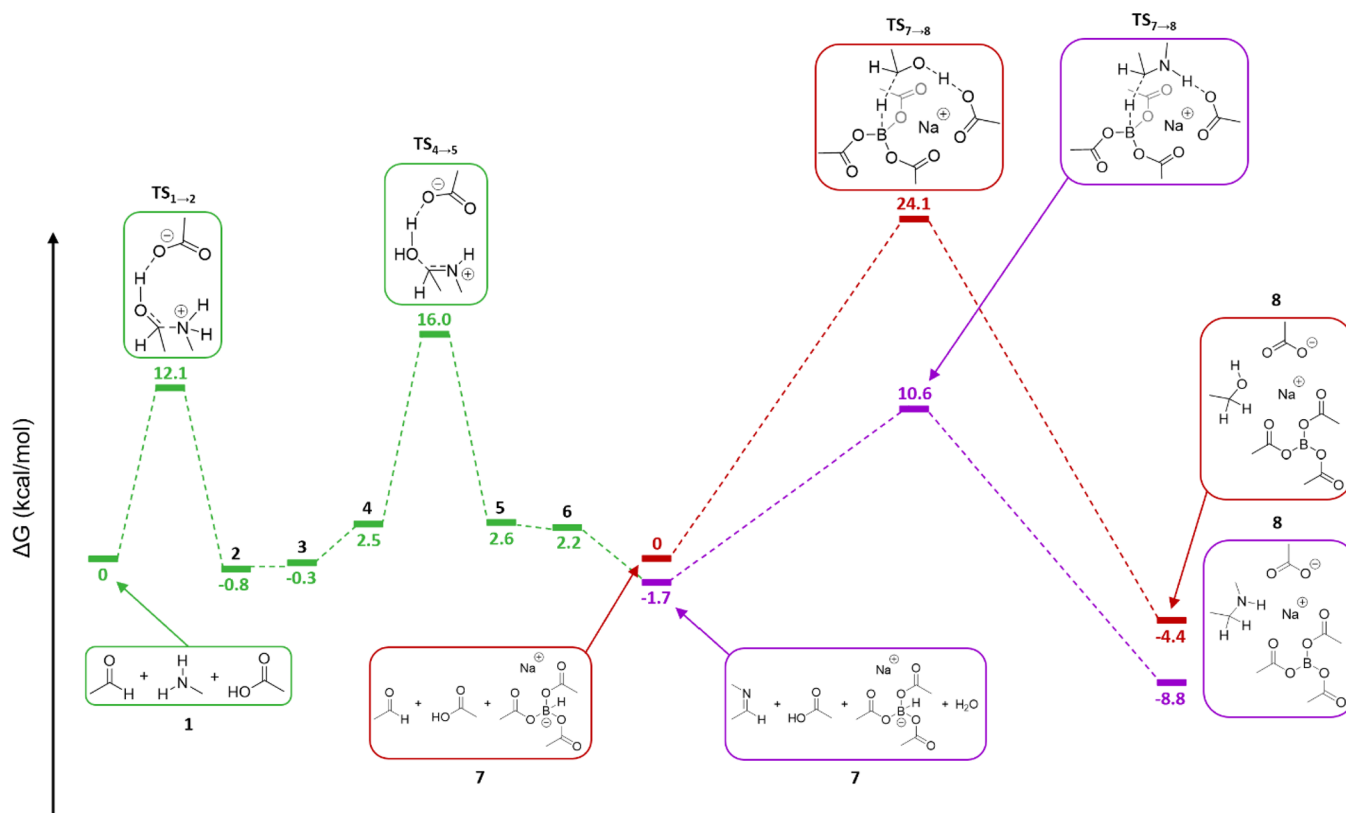
Figure 2. Reaction coordinate diagram for the possible reaction pathways of a direct reductive amination protocol with acetaldehyde and methylamine in DCE. Acetaldehyde can either interact with the methylamine (**1**) or STAB (**3**), with the starting states of these pathways set to zero for comparison. If the acetaldehyde condenses with the methylamine, it will follow the imine formation pathway (green) and then the imine reduction pathway (purple). If acetaldehyde reacts immediately with STAB, it will follow the acetaldehyde reduction pathway (red).
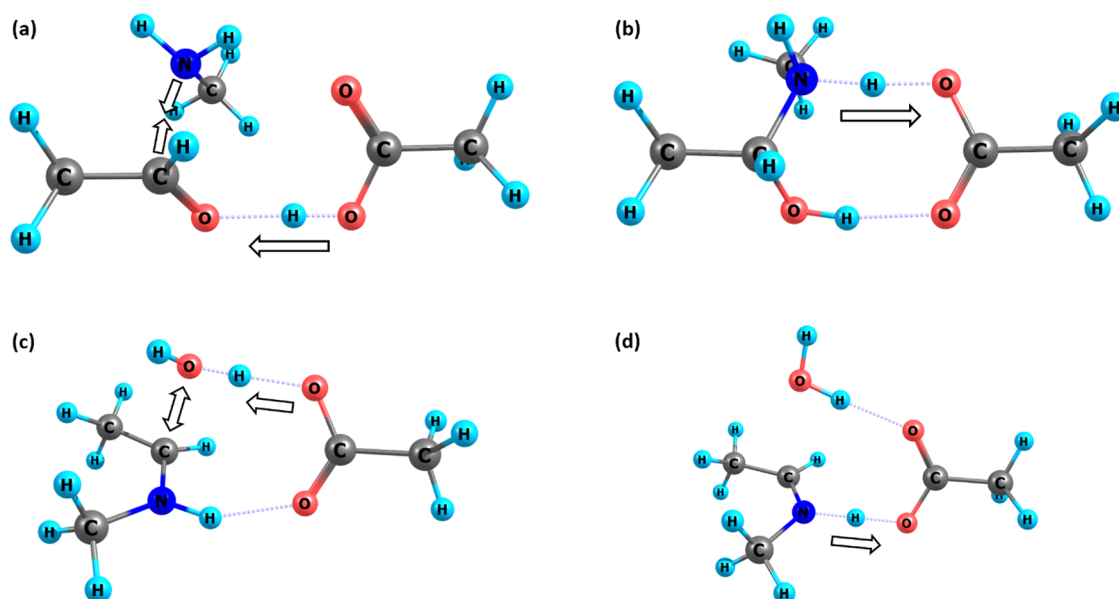
Figure 3. Located transition states for the formation of *Z*-methylethylideneimine with M062X/6-311+G(d,p) and DCE as the solvent. The first transition state entails the formation of the C−N bond (a), followed by the deprotonation of the nitrogen (b). The second transition state involves the elimination of water (c), again followed by the deprotonation of the nitrogen (d).

the hydride-accepting carbonyl carbon in the acetaldehyde reduction is slightly more positive than that on the iminium carbon in the *Z*-aldimine reduction, with APT charges of 1.53 and 1.35 on the carbonyl and iminium carbon, respectively. Additionally, the deformation energy between the ground state

and the transition state is greater in the *Z*-aldimine case than in the acetaldehyde, with enthalpy values of 27.3 and 18.3 kcal/ mol in the *Z*-aldimine and acetaldehyde reduction, respectively. Since the charge distribution and deformation energy were contrary to expectations, the more probable reasons that
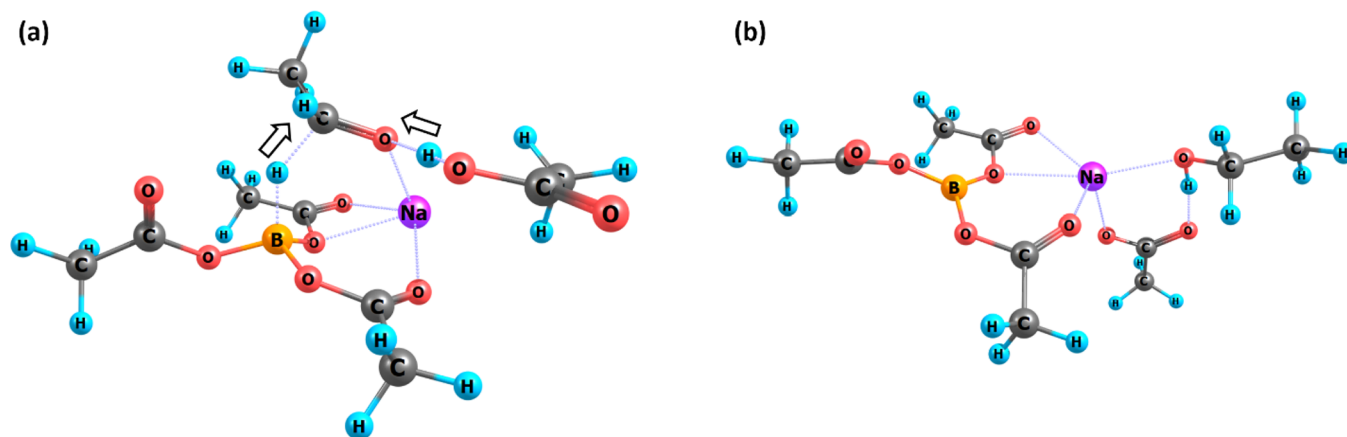
Figure 4. Located transition state (a) and ending complex (b) of the acetaldehyde reduction with M062X/6-311+G(d,p) and DCE as the solvent. Bond distances of Na^+-O in panel (a) range from 2.25 to 2.43 Å. Bond distances of Na^+-O in panel (b) range from 2.22 to 2.46 Å. In panel (a), the $B-H$ and $H-C_{carbonyl}$ distances are 1.33 and 1.38 Å, respectively, while the $OH-O_{carbonyl}$ distance is 1.52 Å.
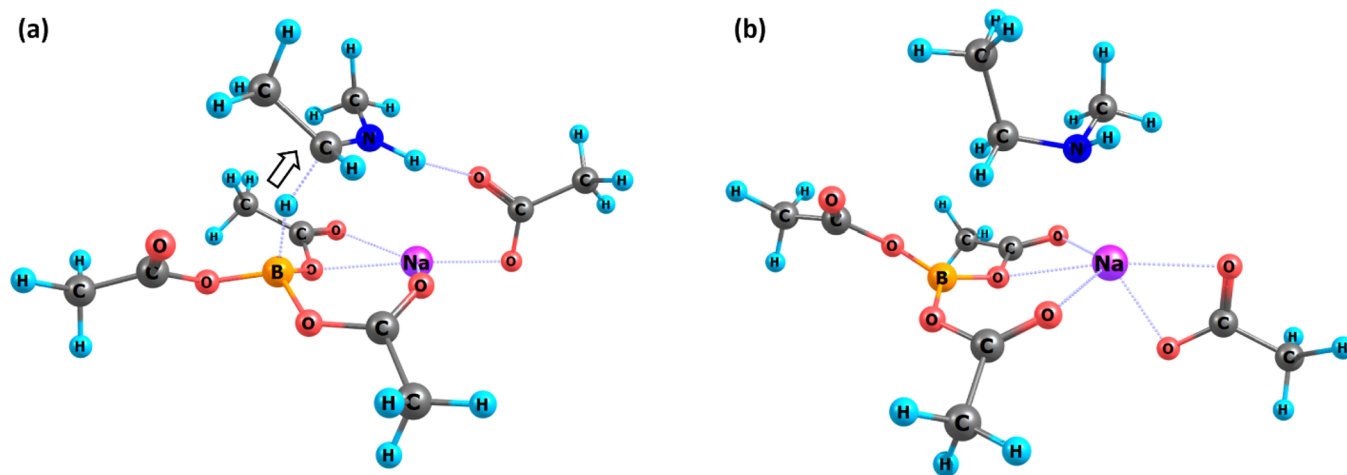
Figure 5. Located transition state (a) and ending complex (b) for Z-methylethylideneimine reduction with M062X/6-311+G(d,p) and DCE as the solvent. Bond distances of Na^+-O in panel (a) range from 2.28 to 2.43 Å. Bond distances of Na^+-O in panel (b) range from 2.31 to 2.49 Å. In panel (a), the $B-H$ and $H-C_{iminium}$ distances are 1.36 and 1.35 Å, respectively, while the $NH-O$ distance is 1.95 Å.

dictate selectivity are bond formation and electrostatic attraction. The transition state for the Z-aldimine reduction is "later" than that for the acetaldehyde reduction as the $C_{iminium}-H_{hydride}$ (1.35 Å) and $N_{iminium}-H_{proton}$ (1.02 Å) bonds are more fully formed in the amine than in the alkoxide, with equivalent $C_{carbonyl}-H_{hydride}$ (1.38 Å) and $O_{carbonyl}-H_{proton}$ (1.52 Å) bonds being less developed. Furthermore, there is greater electrostatic attraction acting on the sodium ion in the Z-aldimine reduction than in the acetaldehyde reduction. In the Z-aldimine reduction, the acetic acid is already deprotonated, yielding acetate, in which the oxygens of the acetate begin to interact with the sodium ion. These electrostatic attractive forces induce additional stability for the Z-aldimine reduction, which is not seen in the acetaldehyde reduction as the acetic acid has not fully deprotonated yet and therefore does not interact with the sodium ion.

The transition states in the imine formation pathway all have a similar structure, adopting a quasi-hexagonal shape. The formation of this six-membered ring pattern begins in the first transition state ($TS_{1\to2}$), with acetic acid approaching an amine proton and carbonyl oxygen. The acetic acid brings the methylamine and acetaldehyde compounds together, facilitat-

ing the initial C−N bond formation, while simultaneously protonating the carbonyl oxygen (Figure 3a). After the C−N bond is formed, the hexagonal shape tightens with the deprotonation of the nitrogen (Figure 3b) and generation of the hemiaminal. The interactions between acetic acid, acetaldehyde, and methylamine are in line with well-known dimeric structures of acetic acid[29−33] and salt bridge formation between acetic acid and amino acids.[34−36] These structures all exhibit a hexagonal shape with the carbon, nitrogen, and oxygen atoms at the vertices and protons passed along the edges. With the formation of the hemiaminal, the second transition state follows ($TS_{4\to5}$), whereupon acetic acid again interacts with the amine proton and hydroxyl oxygen. Acetic acid assists in the elimination of the water group (Figure 3c) by protonating the hydroxyl oxygen as the C−O bond breaks. After the removal of water, the nitrogen is again deprotonated (Figure 3d), releasing the acetic acid, water molecule, and newly formed imine from the hexagonal shape.

The reduction transition states are more complex, with multiple interactions occurring between the substrate (Z-aldimine or acetaldehyde), STAB, and acetic acid. Both located transition states for the reduction step show that the transfer of the hydride is facilitated by Brønsted−Lowry and Lewis acids,
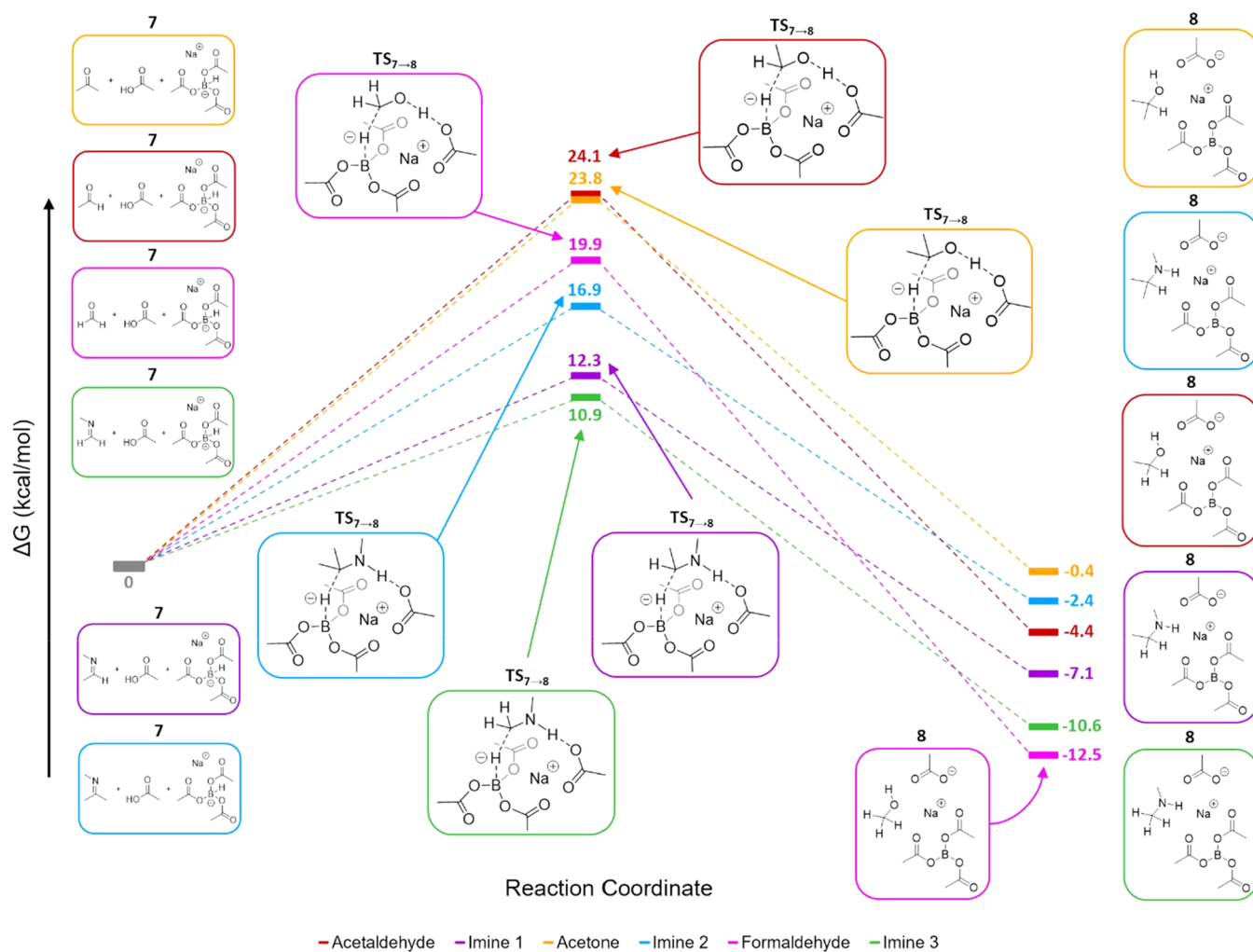
Figure 6. Reaction coordinate diagram for the investigated hydride transfers in DCE, with the acetaldehyde (red), imine 1 (purple), acetone (orange), imine 2 (blue), formaldehyde (pink), and imine 3 (green) represented in the six reaction pathways. Imine 1 refers to *Z*-methylethylideneimine (acetaldehyde + methylamine), imine 2 refers to *N*-methyl-2-propylideneimine (acetone + methylamine), and imine 3 refers to *N*-methylmethanimine (formaldehyde + methylamine).

with the exact coordination geometry slightly altering depending on the substrate. For the acetaldehyde reduction (Figure 4a), the hydride transfer from the boron atom to the carbonyl carbon occurs in tandem with protonation of the carbonyl oxygen by acetic acid. Upon accepting the hydride from the boron, the carbonyl carbon converts to a tetrahedral geometry, while the boron atom adopts a planar geometry.

Another important characteristic of the transition state is the placement of the sodium ion, which holds the three compounds together via ionic interactions with four oxygens. In this regard, the sodium ion acts as a Lewis acid and assembles the structure of the reactants for the hydride transfer. The sodium ion pins two of the acetoxy arms away from the boron center while also lowering the acetaldehyde above the boron, preparing the substrate for hydride acceptance. After the hydride transfer, ethanol (alcohol product), acetate, and triacetoxyboron continue to coordinate around the sodium ion (Figure 4b). In the ending complex, the sodium ion keeps the boron and two of its acetoxy arms in the same plane, while the acetate and ethanol are perpendicular to this plane and coordinate with each other. The ending complex optimizes with triacetoxyboron and free acetate instead of forming tetraacetoxyborate, suggesting that the polarity of the

solvent (DCE) is sufficient to solvate the ionic species within the ending complex. The coordination geometry exhibited by the sodium ion in both the transition state and ending complex is akin to that of crown ether complexes, in particular 15-crown-5 or 18-crown-6.[37−39] The Na$^+$−O bond distances found in both the transition state and ending complex are in the range of 2.2−2.5 Å, which is similar to reported crystal structures of sodium 15-crown-5 complexes.[40,41] In reductive amination protocols, reactions are typically quenched with aqueous basic solutions, especially when acid catalysts are used.[6,7] The complexing behavior around the sodium ion may explain the necessity of aqueous workups, as a salt exchange would be required to isolate the reduced product.

For the reduction of the *Z*-methylethylideneimine (Figure 5a), similar behavior as previously described in the acetaldehyde reduction can be seen. The key difference between the reduction reactions is the behavior of the acetic acid. In the *Z*-aldimine reduction, protonation via acetic acid occurs prior to the hydride transfer instead of being concerted. This behavior can be explained by the higher pK_a of the iminium than that of the protonated aldehyde.

Although the geometry of the transition state and ending complex in the *Z*-aldimine reduction remains similar to the
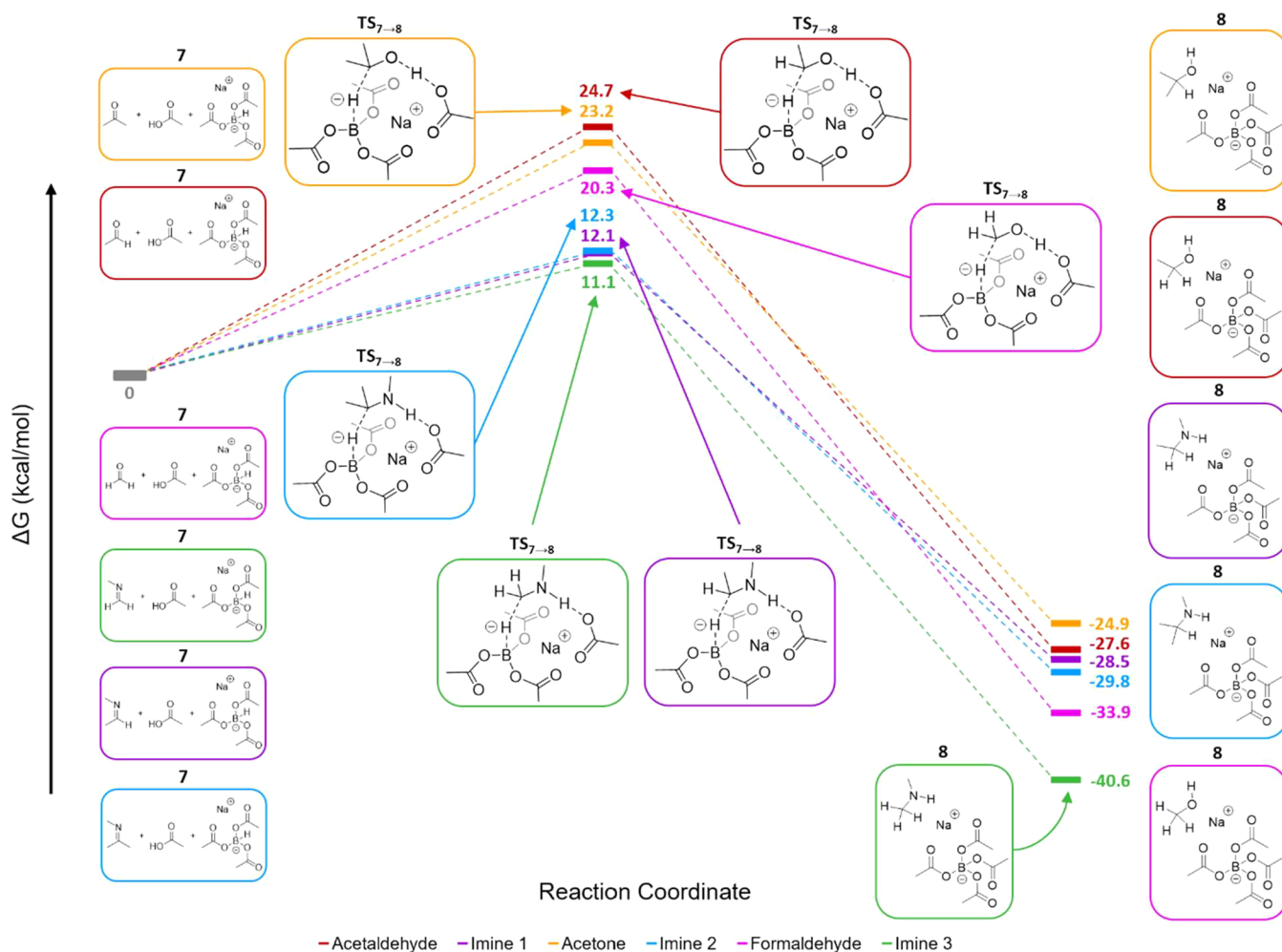
Figure 7. Reaction coordinate diagram for the investigated hydride transfer in THF, with the acetaldehyde (red), imine 1 (purple), acetone (orange), imine 2 (blue), formaldehyde (pink), and imine 3 (green) reductions represented in the six reaction pathways. Imine 1 refers to *Z*-methylethylideneimine (acetaldehyde + methylamine), imine 2 refers to *N*-methyl-2-propylideneimine (acetone + methylamine), and imine 3 refers to *N*-methylmethanimine (formaldehyde + methylamine).

acetaldehyde reduction, the sodium ion does not directly coordinate with *Z*-aldimine or the reduced product. In the transition state (Figure 5a), the *Z*-aldimine is protonated before the transfer of the hydride, with the acetate lowering the iminium above the boron atom and the sodium ion holding the acetate in place. In the ending complex (Figure 5b), the sodium ion does not coordinate with *N*-ethylmethylamine but instead complexes with both acetate oxygens and two arms of the triacetoxyboron. Again, the formation of tetraacetoxyborate is not seen, inferring that DCE can support the acetate and sodium ion species, even without hydrogen bonding as seen in the acetaldehyde reduction. Even though the reduced product does not appear to interact with the sodium ion, an aqueous workup would still be required to remove the sodium ion, acetate, and triacetoxyboron from solution.

Comparison of Reduction Reactions with Form-aldehyde, Acetaldehyde, and Acetone, and Their Respective Imines, in the DCE Solvent. In experiment, the selectivity of STAB has been observed to be sensitive to the nature of the carbonyl compound used, with aldehydes reduced more rapidly than ketones.[12,42,43] Thus, comparison of reduction reactions with formaldehyde, acetaldehyde, and acetone, and their respective imines, would further illuminate the selectivity of STAB. In DCE, it was found that all imine

reductions were both thermodynamically and kinetically favored over their parent carbonyl compound, apart from *N*-methylmethanimine (resultant imine of formaldehyde and methylamine), which was only kinetically favored. In Figure 6, the starting position (**7**) has the substrate (carbonyl or imine compound), acetic acid, and STAB, followed by the hydride transfer transition state ($\mathbf{TS_{7\rightarrow8}}$) where the hydride in the STAB reagent is transferred to the substrate, reducing the substrate to either its alcohol or alkylated amine product. After the reduction step, the reaction pathway falls in energy to the product complexes (**8**).

The activation free energy of all imine derivatives is lower by 6.9−11.8 kcal/mol (34−65%) than that of their parent carbonyl compound, with the addition of methyl groups increasing the activation free energy emerging as a general trend. Similar conclusions can be drawn for the free energy of reaction of the imine derivatives, which is 1.9−2.7 kcal/mol (47−140%) lower than that of their parent carbonyl compound, except for *N*-methylmethanimine (resultant imine from formaldehyde and methylamine). In the *N*-methyl-methanimine case, the free energy of reaction is 1.9 kcal/mol (16%) higher than that for formaldehyde. However, its activation free energy is significantly lower than that for the formaldehyde reduction (9 kcal/mol, 58%); thus, it is still
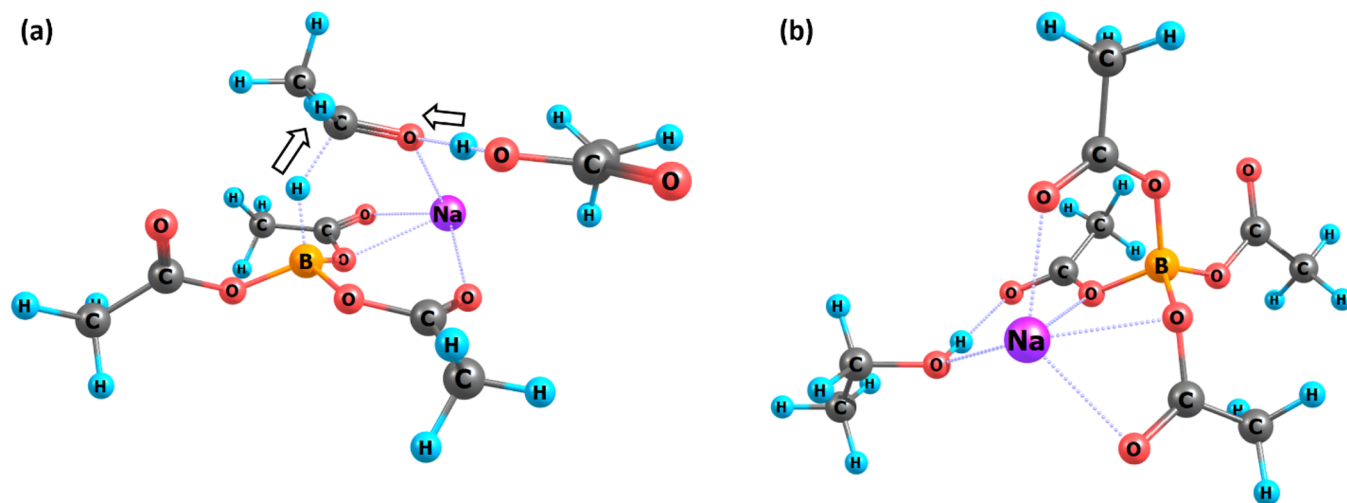
Figure 8. Located transition state (a) and ending complex (b) of the acetaldehyde reduction with M062X/6-311+G(d,p) and THF as the solvent. Bond distances of Na$^+$−O in panel (a) range from 2.25 to 2.43 Å. Bond distances of Na$^+$−O in panel (b) range from 2.24 to 2.45 Å. In panel (a), the B−H and H−C$_{carbonyl}$ distances are 1.33 and 1.37 Å, respectively, while the OH−O$_{carbonyl}$ distance is 1.53 Å.
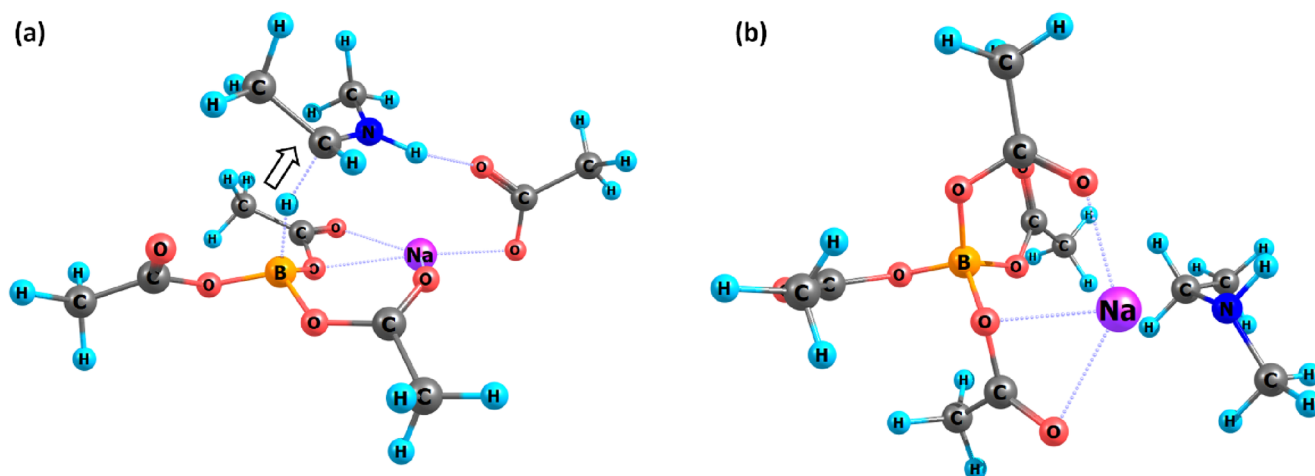
Figure 9. Located transition state (a) and ending complex (b) for Z-methylethylideneimine reduction with M062X/6-311+G(d,p) and THF as the solvent. Bond distances of Na$^+$−O in panel (a) range from 2.28 to 2.44 Å. Bond distances of Na$^+$−O in panel (b) range from 2.25 to 2.38 Å. In panel (a), the B−H and H−C$_{iminium}$ distances are 1.36 and 1.35 Å, respectively, while the NH−O distance is 1.93 Å.

kinetically favored. From either a thermodynamic or kinetic perspective, the hydride transfer to the imine derivatives is more favorable than that of their parent carbonyl compound, supporting the experimentally observed selectivity of STAB. Additionally, although acetone is slightly kinetically favored over acetaldehyde (0.4 kcal/mol, 2%), acetaldehyde is far more thermodynamically favored than acetone (4.0 kcal/mol, 166%). The thermodynamic unfavorability of the acetone reduction is consistent with STAB's selectivity toward aldehydes over ketones reported in the literature. The structural behavior of the located transition states for all reduction reactions is similar to that described previously for the acetaldehyde and Z-aldimine reductions, with form-aldehyde and acetone adopting the same behavior as acetaldehyde and their imine derivatives adopting the same behavior as Z-methylethylideneimine. The transition states, along with their ending complexes, can be found in the Supporting Information.

Thus far, this report has only focused on the (Z)-isomer of methylethylideneimine as past studies on reductive amination using organic hydride donors found that the (Z)-isomer was

more kinetically favored than the (E)-isomer due to a decrease in steric hindrance for the hydride attack.[44,45] Our own DFT calculations align with these studies, as it was found that hydride transfer to the (Z)-isomer of the iminium was slightly kinetically favored by 0.4 kcal/mol over the (E)-isomer.

Solvent Effects on Reduction Reactions: Exchanging the DCE Solvent with THF. Another common solvent used in the literature for reductive amination is tetrahydrofuran (THF); thus, the reduction reactions of formaldehyde, acetaldehyde, and acetone, and their imine derivatives, were also performed using THF model solvation (Figure 7). The reduction reactions in THF adopted similar reaction pathways as in DCE, with the starting position (**7**) having the substrate, acetic acid, and STAB, followed by the hydride transfer (**TS$_{7→8}$**), and then falling in energy to the product complexes (**8**).

In THF, the hydride transfers to the imine derivatives are all thermodynamically and kinetically favored over their parent carbonyl compounds, with the activation free energy being 9.2−12.6 kcal/mol (59−68%) lower and the free energy of reaction being 1.0−6.7 kcal/mol (4−18%) lower. Additionally,

the acetaldehyde reduction is more thermodynamically favored over acetone (2.6 kcal/mol, 10%). Although not shown in Figure 6, *E*-methylethylideneimine was also considered in comparison to *Z*-methylethylideneimine, and it was again found that the hydride transfer to the (*Z*)-isomer was slightly kinetically favored by 0.7 kcal/mol over the (*E*)-isomer.

The most notable difference with the reduction reactions in THF is the ending complexes, where the acetate by-product binds directly to the boron center, forming tetraacetoxyborate (Figures 8 and 9). The sodium ion is encapsulated by the acetoxy arms, forming a cage-like structure around the ion. In the case of the carbonyl compound reductions, the alcohol product also coordinates with the sodium ion. The difference in geometry is likely due to the solvent's dielectric constant (ε), with THF ($\varepsilon = 7.43$) having a lower dielectric constant than DCE ($\varepsilon = 10.1$) and therefore being less able to stabilize electric charge. The cage-like structures seen in the ending complexes are reminiscent of binding sites in transport proteins[46−49] and allosteric pockets of G protein-coupled receptors (GPCRs).[50,51] Such behavior is anticipated as the dielectric constant for the interior of proteins typically falls within 6−7,[52] comparable to that of THF's dielectric constant. Although the ending complexes are optimized into different geometries than for DCE solvation, the transition states in THF have similar motions to the ones located in DCE. The transition states in THF, along with their ending complexes, can be found in the Supporting Information.

Lewis Acid Effects on Reduction Reactions: Exchanging Na⁺ with Li⁺ and K⁺. To investigate the importance of the Lewis acid, calculations of the acetaldehyde and *Z*-methylethylideneimine reduction reactions were performed with lithium or potassium in place of sodium. It was found that the overall geometry of these transition states did not change, with only the ion−oxygen bond distances adjusting to accommodate the ionic radii of the Lewis acid. In the lithium case, the Li⁺−O bond distances were found to be 1.9−2.3 Å, similar to 12-crown-4 complexes, while the potassium case had K⁺−O bond distances in the 2.6−2.7 Å range, similar to 18-crown-6 complexes.[37−39] However, more considerable differences were observed in the activation free energy of these transition states (Tables 1 and 2). For both acetaldehyde and

Table 1. Activation Free Energy of Acetaldehyde Reduction Reactions in Reference to Metal Ions[a]

ion	solvent	
	DCE	THF
lithium	23.8	24.2
sodium	24.1	24.7
potassium	26.1	26.6

[a]Energy values are reported in kcal/mol.

Table 2. Activation Free Energy of *Z*-Methylethylideneimine Reduction Reactions in Reference to Metal Ions[a]

ion	solvent	
	DCE	THF
lithium	10.1	10.4
sodium	12.3	12.1
potassium	16.0	15.9

[a]Energy values are reported in kcal/mol.

Z-aldimine reduction reactions in either DCE or THF, the lithium case required less activation free energy, while potassium required more. The activation free energy for the acetaldehyde reduction with lithium triacetoxyborohydride (LTAB) decreased by 0.3 kcal/mol (1%) and 1.9 kcal/mol (8%) in DCE and THF, respectively. In regard to the acetaldehyde reduction with potassium triacetoxyborohydride (PTAB), the activation free energy increased by 1.9 kcal/mol (8%) in both DCE and THF. As for the *Z*-aldimine reductions, with LTAB, the activation free energy decreased by 2.2 kcal/mol (20%) and 1.7 kcal/mol (16%) in DCE and THF, respectively, and with PTAB, the activation free energy increased by 3.6 kcal/mol (26%) and 3.8 kcal/mol (27%) in DCE and THF, respectively. Changing the Lewis acid has a more significant impact on the *Z*-aldimine reduction than acetaldehyde.

Methylamine−Acetic Acid Equilibrium. A potential issue with the use of an acid catalyst is the acid−base equilibrium between the amine reagent and the acid catalyst. The amine reagent and acid catalyst are often used in similar stoichiometric amounts;[6,7] thus, the acid−base equilibrium may compete with the overall reductive amination reaction. If the basicity of the amine is too strong, or acid catalyst is too strong, then the amine will be protonated and will not be able to perform the nucleophilic attack. Thus, the enthalpy difference between the methylamine and acetic acid adducts was obtained to determine the favorable side of the equilibrium (Scheme 3).

Scheme 3. Methylamine−Acetic Acid Equilibrium
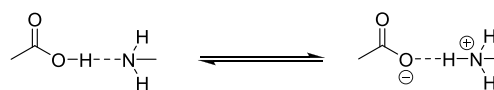
The left side of the methylamine−acetic acid equilibrium was found to be more thermodynamically favorable by 3.5 and 4.9 kcal/mol in DCE and THF, respectively. Also, notably, the methylammonium−acetate adduct did not readily optimize, requiring fixing of the N−H ammonium bond distance (1.033 Å as per Allen *et al.*[53]) to obtain a pseudo-stable geometry. With these calculations, it can be safely assumed that the methylamine would remain unprotonated and therefore will have the ability to perform the nucleophilic attack and start the reductive amination process.

CONCLUSIONS

The acid-catalyzed formation of *Z*-methylethylideneimine from acetaldehyde and methylamine and its subsequent reduction were both found to be thermodynamically and kinetically favored over the acetaldehyde reduction. Despite the mutistep pathway of *Z*-aldimine formation and reduction, all activation free energies and free energies of reactions were lower than those of the reduction of the acetaldehyde, which supports the favorability of the imine reduction observed in experiment. Thus, acetaldehyde will more easily condense with the methylamine than react with STAB in a direct reductive amination protocol. The acid-catalyzed imine formation transition states all exhibited a hexagonal structure, with acetic acid both assembling the reactant structure and providing protons. For the hydride transfer transition state, Brønsted−Lowry and Lewis acids play pivotal roles as they both facilitate the hydride transfer from the STAB reagent to the substrate.

Acetic acid (Brønsted−Lowry) appears to provide stabilization of the end products through protonation, while the sodium ion (Lewis acid) organizes the reactants for the hydride transfer and provides additional stabilization for the end products by coordinating with oxygen atoms. The N−H and C−H bonds in the hydride transfer to iminium in the "late" transition state are more fully formed compared to the O−H and C−H bonds in that to the aldehyde; in addition, sodium-acetate electrostatic attractions are greater in the iminium transition state. These factors account for the lower activation energy for hydride transfer to the iminium.

The additional analysis of the hydride transfer step using formaldehyde, acetaldehyde, and acetone, and their respective imine derivatives, further supports the higher reactivity of the imine, with the imine reductions being either thermodynamically or kinetically favored over their parent carbonyl compound. The structure and motions of the transition states did not significantly change between the substrates, with acetic acid providing the proton source while the sodium ion providing stabilization through coordination with oxygen atoms. The calculations of the reduction reactions performed using the THF model did not display significant differences in the transition sates; however, the geometry of the ending complex did change dramatically. In the ending complexes, acetate directly bonds with the boron center to generate tetraacetoxyborate; such behavior is likely due to THF's lower dielectric constant. As for replacement of the sodium ion with potassium and lithium, it was found that the activation free energies for hydride transfer were lower in the lithium cases but higher in the potassium cases. Although the Lewis acid plays an essential role in the reaction, the investigated reduction reactions are not very sensitive to the identity of the alkali metal.

■ ASSOCIATED CONTENT

Ⓢ Supporting Information

The Supporting Information is available free of charge at https://pubs.acs.org/doi/10.1021/acsomega.2c04056.

> Full Gaussian 16 citation, IRC plots for barrierless proton transfers, and images of optimized transition states not shown in the text (PDF)

> Cartesian coordinates of all calculated structures (XYZ)

■ AUTHOR INFORMATION

Corresponding Author

Robert H. Morris − *Davenport Chemical Research Laboratories, Department of Chemistry, University of Toronto, Toronto, Ontario M5S 3H6, Canada;* ⓞ orcid.org/0000-0002-7574-9388; Email: rmorris@chem.utoronto.ca

Author

Shannon J. Oliphant − *Davenport Chemical Research Laboratories, Department of Chemistry, University of Toronto, Toronto, Ontario M5S 3H6, Canada;* ⓞ orcid.org/0000-0003-1327-7300

Complete contact information is available at:
https://pubs.acs.org/10.1021/acsomega.2c04056

Notes

The authors declare no competing financial interest.

■ REFERENCES

(1) Vardanyan, R. S.; Hruby, V. J. *Synthesis of Best-Seller Drugs*; Academic Press: Amsterdam, 2016.

(2) Lawrence, S. A. *Amines: Synthesis, Properties and Applications*; Cambridge University Press: Cambridge, UK, NY, 2004.

(3) Afanasyev, O. I.; Kuchuk, E.; Usanov, D. L.; Chusov, D. Reductive Amination in the Synthesis of Pharmaceuticals. *Chem. Rev.* **2019**, *119*, 11857−11911.

(4) Roughley, S. D.; Jordan, A. M. The Medicinal Chemist's Toolbox: An Analysis of Reactions Used in the Pursuit of Drug Candidates. *J. Med. Chem.* **2011**, *54*, 3451−3479.

(5) Smith, M. B.; March, J. *March's Advanced Organic Chemistry: Reactions, Mechanisms, and Structure*, 6th ed.; John Wiley & Sons: Hoboken, N.J, 2006.

(6) Abdel-Magid, A. F.; Mehrman, S. J. A Review on the Use of Sodium Triacetoxyborohydride in the Reductive Amination of Ketones and Aldehydes. *Org. Process Res. Dev.* **2006**, *10*, 971−1031.

(7) Abdel-Magid, A. F.; Carson, K. G.; Harris, B. D.; Maryanoff, C. A.; Shah, R. D. Reductive Amination of Aldehydes and Ketones with Sodium Triacetoxyborohydride. Studies on Direct and Indirect Reductive Amination Procedures[1]. *J. Org. Chem.* **1996**, *61*, 3849−3862.

(8) Allegrini, P.; Attolino, E.; Rossi, D. Process for the Preparation of Cinacalcet and Intermediates Thereof. US20110124917A1, May 26, 2011.

(9) Allegrini, P.; Attolino, E.; Rossi, D. A Process for the Preparation of Cinacalcet and Intermediates Thereof. EP2327684B1, October 7, 2015.

(10) Chen, Y.-F.; Henschke, J. P.; Liu, Y.; Chu, G.; Zhang, X. Process and Intermediates for Preparing Lapatinib. EP2550269A1, January 30, 2013.

(11) Xia, G.; Nian, Y.; Yan, T.; Suo, J.; Brand, M.; Arad, O. Novel Process for Preparing Pramipexole and Its Optical Isomeric Mixture by Reduction with Sodium Triacetoxyborohydride. US20060148866A1, July 6, 2006.

(12) Gribble, G. W.; Nutaitis, C. F. Sodium Borohydride in Carboxylic Acid Media. a Review of the Synthetic Utility of Acyloxyborohydrides. *Org. Prep. Proced. Int.* **1985**, *17*, 317−384.

(13) Murugesan, K.; Wei, Z.; Chandrashekhar, V. G.; Neumann, H.; Spannenberg, A.; Jiao, H.; Beller, M.; Jagadeesh, R. V. Homogeneous Cobalt-Catalyzed Reductive Amination for Synthesis of Functionalized Primary Amines. *Nat. Commun.* **2019**, *10*, 5443.

(14) Murugesan, K.; Wei, Z.; Chandrashekhar, V. G.; Jiao, H.; Beller, M.; Jagadeesh, R. V. General and Selective Synthesis of Primary Amines Using Ni-Based Homogeneous Catalysts. *Chem. Sci.* **2020**, *11*, 4332−4339.

(15) Balcells, D.; Nova, A.; Clot, E.; Gnanamgari, D.; Crabtree, R. H.; Eisenstein, O. Mechanism of Homogeneous Iridium-Catalyzed Alkylation of Amines with Alcohols from a DFT Study. *Organometallics* **2008**, *27*, 2529−2535.

(16) Vinogradov, M. M.; Afanasyev, O. I.; Nelyubina, Y. V.; Denisov, G. L.; Loginov, D. A.; Chusov, D. Osmium Catalysis in the Reductive Amination Using Carbon Monoxide as a Reducing Agent. *Mol. Catal.* **2020**, *498*, 111260.

(17) Jameel, F.; Stein, M. The Many Roles of Solvent in Homogeneous Catalysis - The Reductive Amination Showcase. *J. Catal.* **2022**, *405*, 24−34.

(18) Zhao, J.; Liu, S.; Liu, S.; Ding, W.; Liu, S.; Chen, Y.; Du, P. A Theoretical Study on the Borane-Catalyzed Reductive Amination of Aniline and Benzaldehyde with Dihydrogen: The Origins of Chemoselectivity. *J. Org. Chem.* **2022**, *87*, 1194−1207.

(19) Narvariya, R.; Gupta, S.; Jain, A.; Rawal, P.; Gupta, P.; Panda, T. K. One-Pot Reductive Amination of Aromatic Aldehydes in

[Et₃NH][HSO₄] Using Sodium Borohydride and A Mechanistic Investigation Using Computational Method. *ChemistrySelect* **2022**, *7*, No. e202200052.

(20) Frisch, M. J.; Trucks, G. W.; Schlegel, H. B.; Scuseria, G. E.; Robb, M. A.; Cheeseman, J. R.; Scalmani, G.; Barone, V.; Petersson, G. A.; Nakatsuji, H.; Li, X.; Caricato, M.; Marenich, A. V.; Bloino, J.; Janesko, B. G.; Gomperts, R.; Mennucci, B.; Hratchian, H. P.; Ortiz, J. V.; Izmaylov, A. F.; Sonnenberg, J. L.; Williams-Young, D.; Ding, F.; Lipparini, F.; Egidi, F.; Goings, J.; Peng, B.; Petrone, A.; Henderson, T.; Ranasinghe, D.; Zakrzewski, V. G.; Gao, J.; Rega, N.; Zheng, G.; Liang, W.; Hada, M.; Ehara, M.; Toyota, K.; Fukuda, R.; Hasegawa, J.; Ishida, M.; Nakajima, T.; Honda, Y.; Kitao, O.; Nakai, H.; Vreven, T.; Throssell, K.; Montgomery, J. A., Jr.; Peralta, J. E.; Ogliaro, F.; Bearpark, M. J.; Heyd, J. J.; Brothers, E. N.; Kudin, K. N.; Staroverov, V. N.; Keith, T. A.; Kobayashi, R.; Normand, J.; Raghavachari, K.; Rendell, A. P.; Burant, J. C.; Iyengar, S. S.; Tomasi, J.; Cossi, M.; Millam, J. M.; Klene, M.; Adamo, C.; Cammi, R.; Ochterski, J. W.; Martin, R. L.; Morokuma, K.; Farkas, O.; Foresman, J. B.; Fox, D. J. *Gaussian 16*, Revision B.01; Gaussian, Inc.: Wallingford CT, 2016.

(21) Zhao, Y.; Truhlar, D. G. The M06 Suite of Density Functionals for Main Group Thermochemistry, Thermochemical Kinetics, Noncovalent Interactions, Excited States, and Transition Elements: Two New Functionals and Systematic Testing of Four M06-Class Functionals and 12 Other Functionals. *Theor. Chem. Acc.* **2008**, *120*, 215−241.

(22) Marenich, A. V.; Cramer, C. J.; Truhlar, D. G. Universal Solvation Model Based on Solute Electron Density and on a Continuum Model of the Solvent Defined by the Bulk Dielectric Constant and Atomic Surface Tensions. *J. Phys. Chem. B* **2009**, *113*, 6378−6396.

(23) Fukui, K. Formulation of the Reaction Coordinate. *J. Phys. Chem.* **1970**, *74*, 4161−4163.

(24) Fukui, K. The Path of Chemical Reactions - the IRC Approach. *Acc. Chem. Res.* **1981**, *14*, 363−368.

(25) Iwasawa, T.; Hooley, R. J.; Rebek, J., Jr. Stabilization of Labile Carbonyl Addition Intermediates by a Synthetic Receptor. *Science* **2007**, *317*, 493−496.

(26) Jencks, W. P. Studies on the Mechanism of Oxime and Semicarbazone Formation[1]. *J. Am. Chem. Soc.* **1959**, *81*, 475−481.

(27) Cordes, E. H.; Jencks, W. P. On the Mechanism of Schiff Base Formation and Hydrolysis. *J. Am. Chem. Soc.* **1962**, *84*, 832−837.

(28) Raamat, E.; Kaupmees, K.; Ovsjannikov, G.; Trummal, A.; Kütt, A.; Saame, J.; Koppel, I.; Kaljurand, I.; Lipping, L.; Rodima, T.; Pihl, V.; Koppel, I. A.; Leito, I. Acidities of Strong Neutral Brønsted Acids in Different Media. *J. Phys. Org. Chem.* **2013**, *26*, 162−170.

(29) Chocholoušová, J.; Vacek, J.; Hobza, P. Acetic Acid Dimer in the Gas Phase, Nonpolar Solvent, Microhydrated Environment, and Dilute and Concentrated Acetic Acid: Ab Initio Quantum Chemical and Molecular Dynamics Simulations. *J. Phys. Chem. A* **2003**, *107*, 3086−3092.

(30) Beć, K. B.; Futami, Y.; Wójcik, M. J.; Nakajima, T.; Ozaki, Y. Spectroscopic and Computational Study of Acetic Acid and Its Cyclic Dimer in the Near-Infrared Region. *J. Phys. Chem. A* **2016**, *120*, 6170−6183.

(31) Aquino, A. J. A.; Tunega, D.; Haberhauer, G.; Gerzabek, M. H.; Lischka, H. Solvent Effects on Hydrogen Bonds − A Theoretical Study. *J. Phys. Chem. A* **2002**, *106*, 1862−1871.

(32) Mandal, T. K.; Pati, S. K.; Datta, A. Degenerate Intermolecular and Intramolecular Proton-Transfer Reactions: Electronic Structure of the Transition States. *J. Phys. Chem. A* **2009**, *113*, 8147−8151.

(33) Zhang, M.; Chen, L.; Yang, H.; Ma, J. Theoretical Study of Acetic Acid Association Based on Hydrogen Bonding Mechanism. *J. Phys. Chem. A* **2017**, *121*, 4560−4568.

(34) Debiec, K. T.; Gronenborn, A. M.; Chong, L. T. Evaluating the Strength of Salt Bridges: A Comparison of Current Biomolecular Force Fields. *J. Phys. Chem. B* **2014**, *118*, 6561−6569.

(35) Basílio Janke, E. M.; Limbach, H.-H.; Weisz, K. Binding of an Acetic Acid Ligand to Adenosine: A Low-Temperature NMR Study. *J. Am. Chem. Soc.* **2004**, *126*, 2135−2141.

(36) Nagy, P. I.; Erhardt, P. W. Theoretical Studies of Salt-Bridge Formation by Amino Acid Side Chains in Low and Medium Polarity Environments. *J. Phys. Chem. B* **2010**, *114*, 16436−16442.

(37) Pedersen, C. J. Cyclic Polyethers and Their Complexes with Metal Salts. *J. Am. Chem. Soc.* **1967**, *89*, 7017−7036.

(38) Frensdorff, H. K. Stability Constants of Cyclic Polyether Complexes with Univalent Cations. *J. Am. Chem. Soc.* **1971**, *93*, 600−606.

(39) Liou, C.-C.; Brodbelt, J. S. Determination of Orders of Relative Alkali Metal Ion Affinities of Crown Ethers and Acyclic Analogs by the Kinetic Method. *J. Am. Soc. Mass Spectrom.* **1992**, *3*, 543−548.

(40) Watson, K. A.; Fortier, S.; Murchie, M. P.; Bovenkamp, J. W. Crown Ether Complexes Exhibiting Unusual 1:2 Macrocycle Salt Ratios: X-ray Crystal Structures of Cyclohexano-15-Crown-5•2LiOPh, Cyclohexano-15-Crown-5•2NaOPh, and 15-Crown-5•2NaOPh. *Can. J. Chem.* **1991**, *69*, 687−695.

(41) Buchanan, G. W.; Mathias, S.; Bensimon, C.; Charland, J. P. Stereochemistry of Crown Ethers, X-ray Crystallographic Structures, Solid Phase 13C NMR, and Solution Conformational Equilibria in Cis-Syn-Cis Dicyclohexano-15-Crown-5 Ether and Its Sodium Thiocyanate Complex. *Can. J. Chem.* **1992**, *70*, 981−991.

(42) Gribble, G. W. Sodium Borohydride in Carboxylic Acid Media: A Phenomenal Reduction System. *Chem. Soc. Rev.* **1998**, *27*, 395−404.

(43) Gribble, G. W.; Ferguson, D. C. Reactions of Sodium Borohydride in Acidic Media. Selective Reduction of Aldehydes with Sodium Triacetoxyborohydride. *J. Chem. Soc., Chem. Commun.* **1975**, 535−536.

(44) Rothermel, K.; Melikian, M.; Hioe, J.; Greindl, J.; Gramüller, J.; Žabka, M.; Sorgenfrei, N.; Hausler, T.; Morana, F.; Gschwind, R. M. Internal Acidity Scale and Reactivity Evaluation of Chiral Phosphoric Acids with Different 3,3′-Substituents in Brønsted Acid Catalysis. *Chem. Sci.* **2019**, *10*, 10025−10034.

(45) Žabka, M.; Gschwind, R. M. Ternary Complexes of Chiral Disulfonimides in Transfer-Hydrogenation of Imines: The Relevance of Late Intermediates in Ion Pair Catalysis. *Chem. Sci.* **2021**, *12*, 15263−15272.

(46) Gouaux, E.; MacKinnon, R. Principles of Selective Ion Transport in Channels and Pumps. *Science* **2005**, *310*, 1461−1465.

(47) Noskov, S. Y.; Roux, B. Control of Ion Selectivity in LeuT: Two Na⁺ Binding Sites with Two Different Mechanisms. *J. Mol. Biol.* **2008**, *377*, 804−818.

(48) Khafizov, K.; Perez, C.; Koshy, C.; Quick, M.; Fendler, K.; Ziegler, C.; Forrest, L. R. Investigation of the Sodium-Binding Sites in the Sodium-Coupled Betaine Transporter BetP. *Proc. Natl. Acad. Sci. U. S. A.* **2012**, *109*, E3035−E3044.

(49) Loo, D. D. F.; Jiang, X.; Gorraitz, E.; Hirayama, B. A.; Wright, E. M. Functional Identification and Characterization of Sodium Binding Sites in Na Symporters. *Proc. Natl. Acad. Sci. U. S. A.* **2013**, *110*, E4557−E4566.

(50) Katritch, V.; Fenalti, G.; Abola, E. E.; Roth, B. L.; Cherezov, V.; Stevens, R. C. Allosteric Sodium in Class A GPCR Signaling. *Trends Biochem. Sci.* **2014**, *39*, 233−244.

(51) Gutiérrez-de-Terán, H.; Massink, A.; Rodríguez, D.; Liu, W.; Han, G. W.; Joseph, J. S.; Katritch, I.; Heitman, L. H.; Xia, L.; IJzerman, A. P.; Cherezov, V.; Katritch, V.; Stevens, R. C. The Role of a Sodium Ion Binding Site in the Allosteric Modulation of the A2A Adenosine G Protein-Coupled Receptor. *Structure* **2013**, *21*, 2175.

(52) Li, L.; Li, C.; Zhang, Z.; Alexov, E. On the Dielectric "Constant" of Proteins: Smooth Dielectric Function for Macromolecular Modeling and Its Implementation in DelPhi. *J. Chem. Theory Comput.* **2013**, *9*, 2126−2136.

(53) Allen, F. H.; Kennard, O.; Watson, D. G.; Brammer, L.; Orpen, A. G.; Taylor, R. Tables of Bond Lengths Determined by X-ray and Neutron Diffraction. Part 1. Bond Lengths in Organic Compounds. *J. Chem. Soc., Perkin Trans. 2* **1987**, S1−S19.